

## Dark magnetic resonance in an electron-nuclear spin system

R. Rakhmatullin,\* E. Hoffmann,† G. Jeschke,‡ and A. Schweiger§

Laboratorium für Physikalische Chemie, Eidgenössische Technische Hochschule, ETH-Zentrum, CH-8092 Zürich, Switzerland

(Received 14 October 1997)

Dark magnetic resonance in the solid state is observed and is shown to be analogous to electromagnetically induced transparency in coherent optics. The basis of the two effects is coherent population trapping, which can conveniently be described by the product operator formalism. It is demonstrated that pulse electron paramagnetic resonance experiments on electron-nuclear spin systems provide a simple means for studying the physics of these types of coherence phenomena. [S1050-2947(98)07205-9]

PACS number(s): 33.25.+k, 32.30.Dx, 33.35.+r, 76.30.-v

During the last few years, a number of new phenomena in coherent optics like dark resonance, electromagnetically induced transparency, inversionless amplification, and lasing without inversion, have attracted considerable attention [1–11]. In 1993 amplification without population inversion [12,13] and in 1995 lasing without population inversion [14,15] have been demonstrated experimentally on metal vapors. Very recently the first observation of electromagnetically induced transparency in a solid medium has been reported [16]. In laser physics the basic principles of these phenomena are often discussed by means of a three-level atomic system of  $\Lambda$  configuration [1,2,4,5], consisting of an upper level and a low-frequency coherent superposition of two lower sublevels. The transition frequency between upper and lower levels lies in the optical range, whereas the frequency splitting of the two lower levels is in the radio or microwave frequency range.

In this paper we report the observation of dark magnetic resonance on an electron-nuclear spin system. In such a pulse electron paramagnetic resonance (EPR) experiment, the optical electric dipole transitions are replaced by magnetic dipole transitions of the electron spins and the sublevel transition by a magnetic dipole transition of the nuclear spins. The most simple spin system on which to perform such a dark magnetic resonance experiment consists of one electron spin  $S=1/2$  coupled to one nuclear spin  $I=1/2$  subject to an external static magnetic field  $B_0$ . Figure 1(a) shows the four-level diagram with energy levels  $|1\rangle$ ,  $|2\rangle$  ( $\alpha$  electron spin state), and  $|3\rangle$ ,  $|4\rangle$  ( $\beta$  electron spin state). The corresponding EPR stick spectrum shown in Fig. 1(b) consists of the two allowed,  $a$ , EPR transitions  $|1\rangle \rightarrow |3\rangle$  and  $|2\rangle \rightarrow |4\rangle$ , and the two forbidden,  $f$ , EPR transitions  $|1\rangle \rightarrow |4\rangle$  and  $|2\rangle \rightarrow |3\rangle$ .

The theoretical description of dark magnetic resonance is based on the product operator formalism commonly used in magnetic resonance experiments [17]. Relaxation is neglected [17,18]. In the product basis the static high-field rotating frame Hamiltonian in angular frequencies is given by [19]

$$\mathcal{H}_0 = \Omega_S S_z + \omega_I I_z + A S_z I_z + B S_z I_x, \quad (1)$$

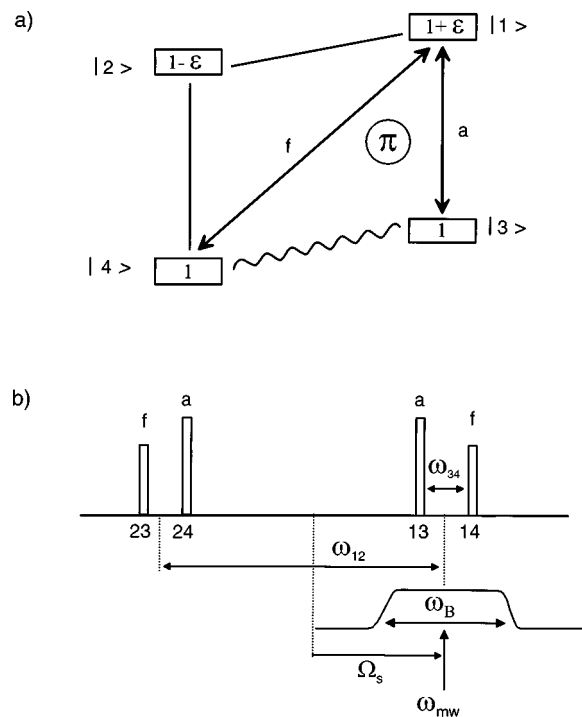


FIG. 1. (a) Energy level diagram of an  $S=1/2$ ,  $I=1/2$  electron-nuclear spin system. Electron spin transitions:  $|1\rangle \rightarrow |3\rangle$ ,  $|2\rangle \rightarrow |4\rangle$ ,  $|1\rangle \rightarrow |4\rangle$ , and  $|2\rangle \rightarrow |3\rangle$ ; nuclear spin transitions:  $|1\rangle \rightarrow |2\rangle$  and  $|3\rangle \rightarrow |4\rangle$ . The two transitions  $|1\rangle \rightarrow |3\rangle$  and  $|1\rangle \rightarrow |4\rangle$  marked by arrows are excited by a semiselective microwave pulse; this leads to creation of nuclear coherence on transition  $|3\rangle \rightarrow |4\rangle$ . The populations illustrate the situation after a semiselective preparation pulse of nominal flip angle  $\pi$ . (b) EPR stick spectrum with two allowed,  $a$ , and two forbidden,  $f$ , electron spin transitions.  $\omega_B$  marks schematically the bandwidth covered by the semiselective pulses;  $\omega_{mw}$  is the microwave carrier frequency and  $\Omega_S$  the resonance offset.

\*Present address: MRS Laboratory, Kazan State University, 420008 Kazan, Russia.

†Present address: SBC Warburg, Europa-Strasse 1, CH-8152 Opfikon, Switzerland.

‡Present address: Max-Planck-Institut Für Polymerforschung, D-55021 Mainz, Germany.

§Author to whom correspondence should be addressed. Address correspondence to Laboratorium für Physikalische Chemie, ETH-Zentrum, 8092 Zürich, Switzerland. FAX: +41-1-632 1021. Electronic address: schweiger@phys.chem.ethz.ch

where  $\Omega_S = \omega_S - \omega_{mw}$  is the offset of the electron Zeeman frequency  $\omega_S = g\beta_e B_0/\hbar$  from the microwave frequency  $\omega_{mw}$ ,  $\omega_I = -g_n\beta_n B_0/\hbar$  is the nuclear Zeeman frequency, and  $A$  and  $B$  are elements of the hyperfine matrix.

The two nuclear transition frequencies in the  $\alpha$  and  $\beta$  electron spin state [Fig. 1(b)] can be expressed as

$$\omega_{12} = \text{sgn}(A + 2\omega_I) \sqrt{(\omega_I + A/2)^2 + (B/2)^2}, \quad (2)$$

$$\omega_{34} = -\text{sgn}(A - 2\omega_I) \sqrt{(\omega_I - A/2)^2 + (B/2)^2}.$$

In the eigenbasis, the Hamiltonian reduces to

$$\mathcal{H}_0 = \Omega_S S_z + \frac{\omega_{12} + \omega_{34}}{2} I_z + (\omega_{12} - \omega_{34}) S_z I_z. \quad (3)$$

During a semiselective microwave pulse of length  $t_p$  along the rotating frame  $x$  axis that simultaneously excites the allowed EPR transition  $|1\rangle \rightarrow |3\rangle$  and the forbidden EPR transition  $|1\rangle \rightarrow |4\rangle$ , the Hamiltonian is given by

$$\mathcal{H}^{(13,14)} = \omega_1 [\sqrt{I_a} S_x^{(13)} - \sqrt{I_f} S_x^{(14)}], \quad (4)$$

with the microwave pumping field amplitude  $\omega_1 = g\beta_e B_1/\hbar$ , the single-transition operators  $S_x^{(13)} = S_x I^\alpha$  (with  $I^\alpha = \frac{1}{2}1 + I_z$ ),  $S_x^{(14)} = S_x I_x - S_y I_y$  [17,19] describing the excitation of transition  $|1\rangle \rightarrow |3\rangle$  and  $|1\rangle \rightarrow |4\rangle$ , and the allowed and forbidden transition probabilities  $I_a$  and  $I_f$ . The bandwidth  $\omega_B$  of the semiselective pulse is marked schematically in Fig. 1(b). During the pulse, the static Hamiltonian, Eq. (1), can be neglected provided the microwave frequency is close to the frequencies of transition  $|1\rangle \rightarrow |3\rangle$  and  $|1\rangle \rightarrow |4\rangle$ . The propagator calculated from the Hamiltonian given in Eq. (4) is found to be [19]

$$P^{(13,14)} = \exp\{-i[\beta_a S_x^{(13)} + \beta_f S_x^{(14)}]\}, \quad (5)$$

where the quantities  $\beta_a = \beta\sqrt{I_a}$  and  $\beta_f = -\beta\sqrt{I_f}$  denote the effective flip angles for the transition  $|1\rangle \rightarrow |3\rangle$  and  $|1\rangle \rightarrow |4\rangle$ , and  $\beta = \omega_1 t_p$  is the nominal flip angle.

We now assume that the spin system can be described by the density matrix in the eigenbasis

$$(\sigma_1) = \begin{pmatrix} \sigma_{11}^{(1)} & 0 & 0 & 0 \\ 0 & \sigma_{22}^{(1)} & 0 & 0 \\ 0 & 0 & \sigma_{33}^{(1)} & \sigma_{34}^{(1)} \\ 0 & 0 & \sigma_{34}^{(1)*} & \sigma_{44}^{(1)} \end{pmatrix}, \quad (6)$$

with the populations  $\sigma_{11}^{(1)}$ ,  $\sigma_{22}^{(1)}$ ,  $\sigma_{33}^{(1)}$ , and  $\sigma_{44}^{(1)}$ , and the nuclear coherence  $\sigma_{34}^{(1)}$ . A suitable preparation sequence to create such a state will be discussed below.

After a semiselective test pulse of flip angle  $\beta_2$  that again excites the transitions  $|1\rangle \rightarrow |3\rangle$  and  $|1\rangle \rightarrow |4\rangle$ , the system is described by the new density matrix

$$(\sigma_2) = \begin{pmatrix} \sigma_{11}^{(2)} & 0 & \sigma_{13}^{(2)} & \sigma_{14}^{(2)} \\ 0 & \sigma_{22}^{(2)} & 0 & 0 \\ \sigma_{13}^{(2)*} & 0 & \sigma_{33}^{(2)} & \sigma_{34}^{(2)} \\ \sigma_{14}^{(2)*} & 0 & \sigma_{34}^{(2)*} & \sigma_{44}^{(2)} \end{pmatrix}. \quad (7)$$

If both transitions are dipole allowed with the same transition probability  $I_a = I_f = \frac{1}{2}$ , we find for the populations

$$\sigma_{11}^{(2)} = \sigma_{11}^{(1)} + \frac{F}{4} (1 - \cos \beta_2),$$

$$\sigma_{22}^{(2)} = \sigma_{22}^{(1)}, \quad (8a)$$

$$\sigma_{33}^{(2)} = \frac{1}{2} (\sigma_{33}^{(1)} + \sigma_{44}^{(1)}) + \frac{1}{2} (\sigma_{33}^{(1)} - \sigma_{44}^{(1)}) \cos \frac{\beta_2}{2}$$

$$- \frac{F}{8} (1 - \cos \beta_2),$$

$$\sigma_{44}^{(2)} = \frac{1}{2} (\sigma_{33}^{(1)} + \sigma_{44}^{(1)}) - \frac{1}{2} (\sigma_{33}^{(1)} - \sigma_{44}^{(1)}) \cos \frac{\beta_2}{2}$$

$$- \frac{F}{8} (1 - \cos \beta_2),$$

for the nuclear coherence

$$\sigma_{34}^{(2)} = \text{Re}(\sigma_{34}^{(1)}) + i \text{Im}(\sigma_{34}^{(1)}) \cos \frac{\beta_2}{2} + \frac{F}{8} (1 - \cos \beta_2), \quad (8b)$$

and for the electron coherences

$$\sigma_{13}^{(2)} = \frac{-i\sqrt{2}}{2} \sin \frac{\beta_2}{2} \left( E + F \cos \frac{\beta_2}{2} \right), \quad (8c)$$

$$\sigma_{14}^{(2)} = \frac{i\sqrt{2}}{2} \sin \frac{\beta_2}{2} \left( -E + F \cos \frac{\beta_2}{2} \right),$$

where

$$E = \sigma_{33}^{(1)} - \sigma_{44}^{(1)} + 2i \text{Im}(\sigma_{34}^{(1)}), \quad (9a)$$

$$F = \sigma_{33}^{(1)} + \sigma_{44}^{(1)} - 2\sigma_{11}^{(1)} - 2\text{Re}(\sigma_{34}^{(1)}). \quad (9b)$$

The condition for dark resonance is fulfilled if the test pulse has no influence whatsoever on the spin system,  $(\sigma_1) = (\sigma_2)$ . This is the case for  $E = F = 0$ , i.e.,

$$\sigma_{33}^{(1)} = \sigma_{44}^{(1)}, \quad (10a)$$

$$\text{Im}(\sigma_{34}^{(1)}) = 0, \quad (10b)$$

$$\sigma_{33}^{(1)} + \sigma_{44}^{(1)} - 2\text{Re}(\sigma_{34}^{(1)}) = 2\sigma_{11}^{(1)}. \quad (10c)$$

The EPR signal given by the expectation value  $\langle S_y(t) \rangle$  vanishes for all times  $t$  after the test pulse. Apart from a difference in sign in Eq. (10c), which is caused by our choice of the  $\Lambda$  configuration ( $|1\rangle$ ,  $|3\rangle$ , and  $|4\rangle$ ) rather than  $|2\rangle$ ,  $|3\rangle$ , and

$|4\rangle$ ), the formulas in Eqs. (10a)–(10c) are identical to the ones found for three-level atomic systems in coherent optics [1,2].

Note that the population of the level  $|1\rangle$  is already trapped for  $F=0$  irrespective of the value of  $E$ . Thus, if condition (10c) is fulfilled, no absorption or emission of microwave quanta can occur. One also finds that the EPR signal *immediately after the test pulse*

$$\langle S_y(t=0) \rangle = \frac{F}{4} \sin \beta_2 \quad (11)$$

is zero in this case. Nevertheless the system can still interact with the field in two ways, if either of the conditions (10a) or (10b) is not fulfilled.

For  $\text{Im}(\sigma_{34}^{(1)}) \neq 0$ , nuclear coherence can be transferred to electron coherence *although all populations are trapped*. The microwave field then drives an entropy transfer between subsystems of the spin system without exchanging energy with it. Alternatively, if  $\sigma_{33}^{(1)} \neq \sigma_{44}^{(1)}$  while the other two conditions are fulfilled, the microwave field appears to drive directly the nuclear transition. This can be considered as a Raman process, the Stokes or anti-Stokes character being established by the sign of the population difference between levels  $|3\rangle$  and  $|4\rangle$ .

If Eqs. (10a) and (10b) are fulfilled, the behavior of the system can be characterized on the basis of Eq. (9b). The following three cases have to be distinguished

$$\sigma_{33}^{(1)} + \sigma_{44}^{(1)} - 2 \text{Re}(\sigma_{34}^{(1)}) = 2\sigma_{11}^{(1)} \quad \text{for dark resonance,} \quad (12a)$$

$$> 2\sigma_{11}^{(1)} \quad \text{for absorption,} \quad (12b)$$

$$< 2\sigma_{11}^{(1)} \quad \text{for emission.} \quad (12c)$$

In an EPR experiment carried out on a free radical at a temperature  $T > 4$  K and a microwave frequency  $\omega_{\text{mw}}/2\pi \approx 9$  GHz (magnetic field  $B_0 \approx 300$  mT for  $g=2$ ), the electron Zeeman term  $\omega_S S_z$  is the dominant interaction, and for the energy eigenvalues we can assume  $\omega_{i0} \ll kT/\hbar$ ,  $i=1, \dots, 4$  (high-field and high-temperature approximation). The density operator at thermal equilibrium is then given by  $\sigma_0 = \mathbb{1} - 2\varepsilon S_z$ , with the unity operator  $\mathbb{1}$  and  $\varepsilon = g\beta_e B_0/kT$ . The small difference in Boltzmann population caused by the nuclear Zeeman and hyperfine interaction is neglected. In contrast to atomic systems in optics, all the energy levels are nearly equally populated at room temperature, with the population difference between the two electron spin states being only the small fraction  $2\varepsilon$  of about 0.1% of the entire population. Since the unity operator is invariant to transformations and does not give rise to observable effects it is usually omitted in magnetic resonance work. However, in order to stress one of the main differences between coherent optics and magnetic resonance, we use here the full equilibrium operator with the populations  $\sigma_{11}^{(0)} = \sigma_{22}^{(0)} = 1 - \varepsilon$  and  $\sigma_{33}^{(0)} = \sigma_{44}^{(0)} = 1 + \varepsilon$ .

We now assume that, as a result of a suitable preparation of the system, the populations and the nuclear coherence are

given by  $\sigma_{11}^{(1)} = 1 - \varepsilon + \delta$ , with  $0 \leq \delta \leq 2\varepsilon$ ,  $\sigma_{22}^{(1)} = 1 - \varepsilon$ ,  $\sigma_{33}^{(1)} = \sigma_{44}^{(1)} = 1$ , and  $\sigma_{34}^{(1)} = \varepsilon e^{-i\omega_{34}t}$ , respectively. Experimentally, such a state can be prepared, for example, by a semiselective microwave  $\pi$  pulse that simultaneously excites transition  $|1\rangle \rightarrow |3\rangle$  and  $|1\rangle \rightarrow |4\rangle$ , followed by a radio-frequency pulse with a flip angle  $0 \leq \beta_{\text{rf}} \leq \pi$  on-resonant with the nuclear transition  $|1\rangle \rightarrow |2\rangle$  (surviving nuclear coherence on this transition can be eliminated by a phase cycle). By inserting these matrix elements in Eqs. (12a)–(12c) we find the conditions

$$\cos(\omega_{34}t) = \frac{\varepsilon - \delta}{\varepsilon} \quad \text{for dark resonance,} \quad (13a)$$

$$< \frac{\varepsilon - \delta}{\varepsilon} \quad \text{for absorption,} \quad (13b)$$

$$> \frac{\varepsilon - \delta}{\varepsilon} \quad \text{for emission.} \quad (13c)$$

For  $\delta=0$ , we have  $\sigma_{11}^{(1)} = 1 - \varepsilon$ , and dark resonance manifests at time

$$t = \frac{2\pi n}{\omega_{34}}. \quad (14)$$

For  $t \neq 2\pi n/\omega_{34}$ , the spin system absorbs energy. For  $0 < \delta < 2\varepsilon$ , the system can emit energy. The length of the time intervals for emission increases with increasing  $\delta$ . In the interval  $0 < \delta < \varepsilon$  the population  $\sigma_{11}^{(1)} = 1 - \varepsilon + \delta$  is always *smaller* than the population of the levels in the ground state,  $\sigma_{33}^{(1)} = \sigma_{44}^{(1)} = 1$ , and *amplification without inversion* takes place during the emission periods. If in addition the spin system together with the resonant structure fulfills the maser condition [20], *masing without inversion* will be observed. For  $\varepsilon < \delta \leq 2\varepsilon$ , the time intervals for which emission is observed further increase but for these  $\delta$  values always emission *with inversion* is observed.

Note that in the context of coherent population trapping, the term ‘‘inversion’’ always means population inversion in the *eigenbasis* of the unperturbed Hamiltonian. This choice of the basis ensures that populations are constants of motion in the absence of an external perturbation. For the case of ‘‘inversionless amplification’’ it has been demonstrated that another representation can be found where inversion exists [12]. That the inversion is actually only hidden can be seen from the fact that in any system fulfilling condition (12c) the transfer of the coherence on the *low-frequency* transition  $|3\rangle \rightarrow |4\rangle$  to polarization by a  $\pi/2$  pulse along the  $y$  axis would create population inversion on one of the *high-frequency* transitions,  $|1\rangle \rightarrow |3\rangle$  or  $|1\rangle \rightarrow |4\rangle$ .

For the description of the dark magnetic resonance experiment the situation with  $\delta=2\varepsilon$ ,  $\sigma_{11}^{(1)} = 1 + \varepsilon$ , is of particular interest. Such a state can easily be prepared by applying only a semiselective  $\pi$  pulse that excites the two transitions  $|1\rangle \rightarrow |3\rangle$  and  $|1\rangle \rightarrow |4\rangle$ . The dark resonance condition is then fulfilled for

$$t = \frac{(2n+1)\pi}{\omega_{34}}, \quad (15)$$

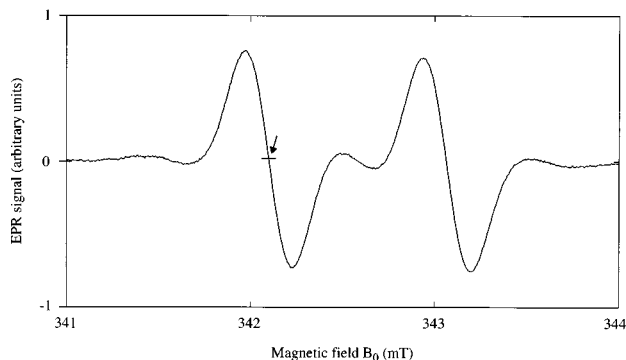


FIG. 2. Room temperature continuous wave EPR spectrum of a  $\gamma$ -irradiated potassium hydrogen malonate single crystal, oriented for minimum  $\omega_{34}$  nuclear transition frequency. The arrow marks the observer position used for the dark magnetic resonance experiment.

and occurs periodically at time intervals

$$T = 2\pi/\omega_{34}. \quad (16)$$

A single crystal of  $\gamma$ -irradiated potassium hydrogen malonate (10 kGy) is used to demonstrate dark magnetic resonance. The irradiation product, the free radical  $^-\text{OOC}-\text{CH}-\text{COO}^-$ , is oriented in the same way as the undamaged molecule with one principal axis of the  $\alpha$ -proton hyperfine matrix along the crystallographic twofold symmetry axis  $b$  [21]; site splitting is therefore absent for all orientations of the magnetic field. The unpaired electron and the spin of the  $\alpha$  proton represent an  $S=1/2$ ,  $I=1/2$  four-level electron-nuclear spin system with an orthorhombic hyperfine matrix with principal values  $-27.4$ ,  $-56.3$ , and  $-86.3$  MHz [21]. The hyperfine interactions of the protons of neighboring hydrogen malonate molecules are much smaller and have virtually no influence on the dark magnetic resonance effect. The experiment has been carried out at room temperature on a Bruker ESP 380E pulse EPR spectrometer operating at 9.7 GHz. An orientation of the crystal was chosen for which the nuclear transition frequency  $\omega_{34}$  was close to minimum. For this particular orientation the transition probabilities of all four EPR transitions are the same,  $I_a = I_f = \frac{1}{2}$ .

The continuous wave EPR spectrum shown in Fig. 2 consists of two inhomogeneously broadened lines of width  $(\Delta\Omega_S)_{1/2} = 0.25$  mT separated by 0.97 mT (corresponding to  $\omega_{12}/2\pi = 27.08$  MHz). The small splitting of  $\omega_{34}/2\pi = 1.45$  MHz (0.052 mT) is not resolved. The experiment was carried out at the center of the low-field line, marked by an arrow [high-frequency lines in Fig. 1(b)] i.e., only the energy levels  $|1\rangle$ ,  $|3\rangle$ , and  $|4\rangle$ , representing a  $\Lambda$  configuration are involved in the experiment. The microwave pulse sequence is shown in Fig. 3. The semiselective pulse of length  $t_{p1} = 192$  ns and nominal flip angle  $\beta = \pi$  simultaneously excites the two EPR transitions  $|1\rangle \rightarrow |3\rangle$  and  $|1\rangle \rightarrow |4\rangle$  with equal transition probability and creates nuclear coherence on the low-frequency transition  $|3\rangle \rightarrow |4\rangle$ . After free evolution of time  $t$ , a two-pulse echo sequence  $\pi/2-\tau-\pi-\tau$ -echo, consisting of a semiselective pulse of length  $t_{p1} = 192$  ns and nominal flip angle  $\pi/2$ , a time delay  $\tau = 750$  ns, and a nonselective  $\pi$  pulse of length  $t_\pi = 16$  ns, is used to monitor the state of the three-level quantum system. Echo rather than free induction decay

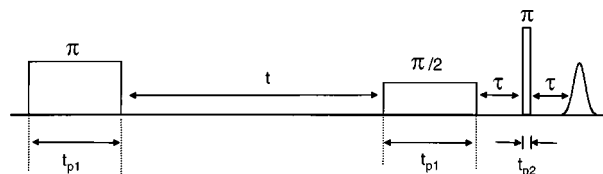


FIG. 3. Pulse sequence for the observation of dark magnetic resonance consisting of a semiselective preparation pulse of flip angle  $\pi$  and a two-pulse echo detection sequence.

detection is used since the free induction decay cannot be observed due to the spectrometer deadtime. According to Eq. (16) dark resonance or population trapping should manifest in time intervals of  $T = 2\pi/\omega_{34} = 690$  ns. At these times, the spin system is *transparent* for the semiselective  $\pi/2$  pulse and the echo intensity is zero.

The experimental echo amplitude recorded as a function of time  $t$  is shown in Fig. 4(a). The phase cycle  $[0] + [\pi]$  of the semiselective  $\pi$  pulse eliminates residual electron coherence present after the first pulse. In addition, the base line obtained without microwave pulses has been subtracted. A repetition rate of 250 Hz has been used. Since the sequence is closely related to an inversion recovery experiment, the sign of the echo amplitude is chosen to be positive for  $t \rightarrow \infty$ . As predicted, dark resonance effects are observed in time intervals of  $T = 690$  ns (first four events marked by arrows). Because of spin lattice relaxation the echo amplitude is zero only for the first population trapping event (bold arrow). For the subsequent events the echo signals approach

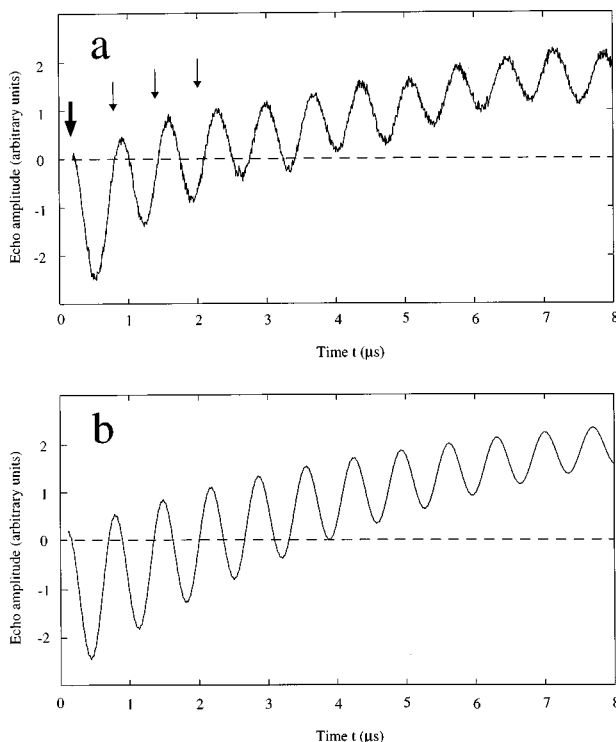


FIG. 4. (a) Experimental demonstration of dark magnetic resonance on a  $\gamma$ -irradiated potassium malonate single crystal at room temperature. The echo amplitude is recorded as a function of time  $t$  between preparation and detection. The arrows mark the first four dark resonance events occurring in time intervals of 690 ns. (b) Numerical simulation of the experimental time trace shown in (a).

asymptotically the value obtained without a preparation pulse. In addition the modulation amplitude of the echo decreases with increasing time  $t$  due to the loss in phase memory of the nuclear spins. The shift of the echo modulation trace of about 145 ns to shorter times compared to the values predicted by Eq. (15) is caused by the finite length of the two semiselective pulses. Fig. 4(b) shows a numerical simulation of the experimental time trace. All the features are nicely reproduced for a spin lattice relaxation time  $T_{1e} \approx 5 \mu\text{s}$ , and a nuclear phase memory time  $T_{2n} \approx 8 \mu\text{s}$ .

Population trapping by coherences cannot only be demonstrated by an especially designed EPR experiment, it is actually an unrecognized feature of a number of existing pulse EPR schemes. For example, in the three-pulse electron spin echo envelope modulation experiment,  $\pi/2$ - $\tau$ - $\pi/2$ - $T$ - $\pi/2$ - $\tau$ -echo, on an  $S=1/2$ ,  $I=1/2$  spin system with semiselective pulses again exciting the transitions  $|1\rangle \rightarrow |3\rangle$  and  $|1\rangle \rightarrow |4\rangle$ , the preparation sequence  $\pi/2$ - $\tau$ - $\pi/2$ , creates nuclear coherence on the  $|3\rangle \rightarrow |4\rangle$  transition that evolves during time  $T$ . The echo amplitude is given by [22]

$$E(\tau, T) = 1 - \frac{k}{2} \left[ 1 - \frac{1}{2} \cos(\omega_{34}\tau) + \cos[\omega_{34}(\tau + T)] \right] \quad (17)$$

with  $k=4I_a I_f$ . For  $\tau=(2n+1)\pi/\omega_{34}$  and  $k=1$  the system is prepared in a state where condition (10c) is fulfilled, so that the population of level  $|1\rangle$  is trapped. This state recurs for  $T=2m\pi/\omega_{34}$ . Although coherences on the two electron spin transitions are still created by the transfer from nuclear coherence and by the Raman process, they cancel each other at the time where echo formation would be expected.

In more common experiments, population and coherence trapping situations are more complex, since at least four energy levels corresponding to a double  $\Lambda$  configuration are involved. Such cases that can again be described by the product operator formalism in a transparent and straightforward way will be discussed elsewhere. An electron spin echo modulation sequence, where in the view of our new insight the population trapping situation is still a rather simple one, has recently been proposed by Borbat *et al.* [23].

We now briefly summarize the main differences between coherent optics and magnetic resonance experiments related

to population trapping. The frequency of the dark resonance phenomenon reported in this paper is about a factor  $5 \times 10^4$  lower than the one in the optical experiments. In contrast to optics, the energy levels are nearly equally populated and the amplitudes of the electron and nuclear coherences are determined by the population *differences* rather than by the populations. The wavelength used in an EPR experiment is usually larger than the size of the sample. However, with a suitable experimental setup, it should be possible to observe electromagnetically induced transparency also in magnetic resonance, similar to microwave self-induced transparency [24]. Amplification without inversion occurs in both frequency regimes and lasing without inversion finds its analogon in *masing without inversion*.

In conclusion we have demonstrated that dark magnetic resonance can be observed in four-level electron-nuclear spin systems. For the description of the phenomenon, we used a well developed quantum mechanical formalism that is common in magnetic resonance work and that can easily be extended to more complex spin systems. Powerful tools like the computer package GAMMA [25] that are based on this formalism are now available for detailed numerical computations of the effects. The work presented in this paper once again demonstrates the close relationship between the concepts of magnetic resonance and quantum optics [26]. Most of the new optical phenomena that are based on population trapping can also be observed in spin systems; in particular it should be possible to design and construct a maser without inverting the populations of the electron spins. Magnetic resonance spectroscopy is particularly well suited for the study of the underlying principles of these coherent effects, since the experiments are straightforward and can be easily performed on commercial spectrometers at room temperature. In retrospect, we would like to stress that partial trapping of populations is a feature of a sizable number of widely used pulse magnetic resonance experiments, though it has not been recognized before the optical community described the phenomenon.

We thank Walter Lämmler for the preparation of the potassium hydrogen malonate single crystal. Financial support from the Swiss National Science Foundation is acknowledged.

- 
- [1] Ya. I. Khanin and O. A. Kocharovskaya, J. Opt. Soc. Am. B **7**, 2016 (1990).  
 [2] O. A. Kocharovskaya, Phys. Rep. **219**, 175 (1992).  
 [3] M. O. Scully, Phys. Rep. **219**, 191 (1992).  
 [4] P. Mandel, Contemp. Phys. **34**, 235 (1993).  
 [5] M. O. Scully and M. Fleischhauer, Science **263**, 337 (1994).  
 [6] S. E. Harris, Phys. Today **50** (7), 36 (1997).  
 [7] O. Kocharovskaya and P. Mandel, Quantum Opt. **6**, 217 (1994).  
 [8] J. E. Field, K. H. Hahn, and S. E. Harris, Phys. Rev. Lett. **67**, 3062 (1991).  
 [9] H. Y. Ling, Y.-O. Li, and M. Xiao, Phys. Rev. A **53**, 1014 (1996).  
 [10] C. Peters and W. Lange, Appl. Phys. B: Lasers Opt. **62**, 221 (1996).  
 [11] P. B. Sellin, G. A. Wilson, K. K. Meduri, and T. W. Mossberg, Phys. Rev. A **54**, 2402 (1996).  
 [12] W. E. van der Veer, R. J. J. van Diest, A. Dönszelmann, and H. B. van Linden van den Henvell, Phys. Rev. Lett. **70**, 3243 (1993).  
 [13] A. Nottelmann, C. Peters, and W. Lange, Phys. Rev. Lett. **70**, 1783 (1993).  
 [14] A. S. Zibrov, M. D. Lukin, D. E. Nikonov, L. Hollberg, M. O. Scully, V. L. Velichansky, and H. G. Robinson, Phys. Rev. Lett. **75**, 1499 (1995).  
 [15] G. G. Padmabandu, G. R. Welch, I. N. Shubin, E. S. Fry, D. E.

- Nikonov, M. D. Lukin, and M. O. Scully, *Phys. Rev. Lett.* **76**, 2053 (1996).
- [16] Y. Zhao, C. Wu, B.-S. Ham, M. K. Kim, and E. Awad, *Phys. Rev. Lett.* **79**, 641 (1997).
- [17] R. R. Ernst, G. Bodenhausen, and A. Wokaun, *Principles of Nuclear Magnetic Resonance in One and Two Dimensions* (Clarendon Press, Oxford, 1987).
- [18] In principle relaxation can be considered by extending our approach to Liouville space and including a relaxation superoperator.
- [19] E. C. Hoffmann, M. Hubrich, and A. Schweiger, *J. Magn. Reson., Ser. A* **117**, 16 (1995).
- [20] A. E. Siegman, *An Introduction to Lasers and Masers* (McGraw-Hill, New York, 1971).
- [21] A. Colligiani, C. Pinzino, M. Brustolon, and C. Corvajo, *J. Magn. Reson.* **32**, 419 (1978).
- [22] S. A. Dikanov and Yu. D. Tsvetkov, *Electron Spin Echo Envelope Modulation (ESEEM) Spectroscopy* (CRC Press, Boca Raton, 1992).
- [23] P. P. Borbat and A. M. Raitsimring, *J. Magn. Reson., Ser. A* **114**, 261 (1995).
- [24] S. B. Grossman and E. Hahn, *Phys. Rev. A* **14**, 2206 (1976).
- [25] S. A. Smith, T. O. Levante, B. H. Meier, and R. R. Ernst, *J. Magn. Reson., Ser. A* **106**, 75 (1994).
- [26] E. L. Hahn, *Concepts Magn. Reson.* **9**, 69 (1997).